Thermal transport in materials with disclination dipoles and disclination loops

2002 J. Phys.: Condens. Matter 14 12923

(http://iopscience.iop.org/0953-8984/14/48/334)

INSTITUTE OF PHYSICS PUBLISHING JOURNAL OF PHYSICS: CONDENSED MATTER

J. Phys.: Condens. Matter **14** (2002) 12923–12928 PII: S0953-8984(02)53995-3

Thermal transport in materials with disclination dipoles and disclination loops

S E Krasavin[1] **and V A Osipov**

Joint Institute for Nuclear Research, Bogoliubov Laboratory of Theoretical Physics, 141980 Dubna, Moscow Region, Russia

E-mail: krasavin@thsun1.jinr.ru

Received 27 September 2002
Published 22 November 2002
Online at stacks.iop.org/JPhysCM/14/12923

Abstract
The problem of phonon scattering by static strain fields due to biaxial wedge disclination dipoles (WDDs) of finite length and circular wedge disclination loops (WDLs) is studied in the framework of the deformation potential approach. The specific behaviour of the thermal conductivity, κ, is found for both defects. In particular, for WDDs the crossover from T^2 to T is predicted at low temperatures. For circular WDLs, $\kappa(T)$ exhibits a minimum at some temperature T^* in the low-temperature range. Above T^* $\kappa \sim T^2$ (dislocation-like behaviour), while below T^*, one finds $\kappa \sim T^{-3}$.

1. Introduction

The role of dislocations in electron transport in semiconductors is widely recognized now (see, e.g., [1]). Dislocations serve as effective scattering centres for conducting electrons, thus resulting in a dislocation-induced contribution to the transport characteristics [2]. In contrast, the contribution to the conductivity in semiconductors due to rotational dislocations (disclinations) is not yet well understood. At the same time, the theoretical consideration proposed in [3, 4] shows the importance of disclinations in semiconductors.

Some aspects of the electron scattering due to straight wedge disclinations have been considered in [5] where a noticeable difference between the electronic properties of dislocations and disclinations was found—namely, while dislocations can grasp electrons on the localized levels in the core region, for negative disclinations only resonance-like electron states can exist. Also, the behaviour of the residual resistivity in simple metals caused by arrays of wedge disclinations was investigated in [6] (as a function of the density of defects n). It was shown that the n-dependence of the residual resistivity deviates from the linear law over a wide range of defect densities unlike in the case of dislocations. In real crystals, however, wedge and twist disclinations are combined in groups (dipoles, multipoles, loops) forming screened

[1] Author to whom any correspondence should be addressed.

0953-8984/02/4812923+06$30.00

systems [7]. A qualitative analysis of the resistivity of metals caused by electron scattering due to the static strain fields of wedge disclination dipoles (WDDs) (both biaxial and uniaxial types) has been presented in [8]. At the same time, the main question of whether disclination dipoles and disclination loops (widely present in materials with rotational plasticity) affect electron mobility in semiconductors (like dislocations) still remains to be answered.

As a first step, in this paper we study the problem of phonon scattering by biaxial WDDs of finite length and by circular wedge disclination loops (WDLs) in the framework of the deformation potential approach [2, 9]. These defects are the simplest screened systems among numerous extended defects in materials with rotational plasticity. The interest in finite WDDs has been aroused by the fact that they can be part of more realistic objects in crystals (e.g. rectangular disclination loops). In turn, disclination loops are strongly screened systems which seem to be the most commonly encountered elements in the majority of real media. Moreover, the long-range strain fields caused by WDDs were found to match those from finite walls of edge dislocations (see, e.g., [10]), while low-angle grain boundaries can be described as dislocation walls. For this reason, the WDD-based model can be applied to interpret the recent experiments [11] on glass-like thermal transport in polycrystalline semiconductors. Note that the problem of phonon scattering due to infinite WDDs has been considered in [10].

2. Model

A mean free path of phonons of frequency ω scattered by the potential associated with a static deformation of a lattice caused by WDDs is calculated within the generally accepted deformation potential approach (see, e.g., [9]). An effective perturbation energy of phonons due to the strain fields caused by WDDs or circular WDLs is

$$U(\boldsymbol{r}) = \hbar\omega\gamma \,\mathrm{Tr}\, E_{ij}, \tag{1}$$

where Tr E_{ij} is the trace of the strain tensor due to WDDs or WDLs, $\hbar\omega$ is the phonon energy, γ is the Grüneisen constant.

Consider the geometry for WDDs and WDLs, where disclination lines of finite length $2d$ of WDDs are directed along the z-axis with coordinates $(\pm L, 0)$ in $z = 0$ plane ($2L$ is the dipole separation). The rotation vectors (Frank vectors) are $\boldsymbol{\Omega_1} = \Omega \boldsymbol{e_z}$ and $\boldsymbol{\Omega_2} = -\Omega \boldsymbol{e_z}$ for disclinations $(-L, 0)$ and $(L, 0)$, respectively; a circular wedge loop of radius R is located in the $z = 0$ plane with a rotation vector $\boldsymbol{\Omega} = \Omega \boldsymbol{e_y}$.

By using the explicit form of the strain fields of WDDs and WDLs (which can be taken from [12, 13]) in equation (1), one can calculate the matrix scattering element in the Born approximation [9, 10]. The results are as follows for WDDs:

$$\begin{aligned}\langle \boldsymbol{k}|U(r)|\boldsymbol{k}'\rangle &= \frac{2A}{V}\frac{\sin(q_z d)}{q_z} \\ &\quad\times \int_0^\infty r\,\mathrm{d}r \int_0^{2\pi} \mathrm{d}\phi\, (K_0(q_z\rho_-) - K_0(q_z\rho_+)) \exp[\mathrm{i} q_\perp r \cos(\phi - \alpha)],\end{aligned} \tag{2}$$

and for WDLs:

$$\langle \boldsymbol{k}|U(r)|\boldsymbol{k}'\rangle = -4\pi \mathrm{i} R^2 \cos\alpha \frac{A}{V}\frac{q_\perp}{q_\perp^2 + q_z^2} J_2(q_\perp R), \tag{3}$$

where $A = \hbar k v_s \gamma \nu (1 - 2\sigma)/(1 - \sigma)$, $\nu = \Omega/2\pi$, σ is the Poisson constant, $K_0(x)$ and $J_2(x)$ are the modified Bessel function and the Bessel function of the first kind, respectively, $\rho_\pm^2 = r^2 \pm 2rL\cos\phi + L^2$, α defines the angle between $\boldsymbol{q}_\perp = (q_x, q_y)$ and the x-axis.

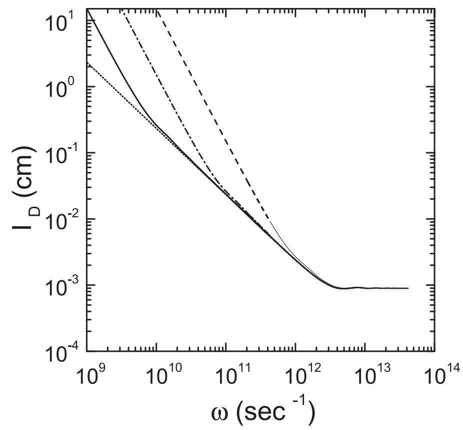

Figure 1. The phonon mean free path l_{WDD} due to scattering on static strain fields of finite biaxial WDDs as a function of frequency for $d = \infty$ (dotted curve), $d = 10^{-4}$ cm (solid curve), $d = 10^{-5}$ cm (dotted–dashed curve), $d = 10^{-6}$ cm (dashed curve). The parameter set used is: $L = 10^{-7}$ cm, $\nu = 0.1$, $n_d = 2 \times 10^{11}$ cm^{-3}, $v_s = 4 \times 10^5$ cm s^{-1}, $B = 4 \times 10^{-3}$.

We consider the elastic scattering with $q = |\boldsymbol{q}| = |\boldsymbol{k} - \boldsymbol{k}'| = 2k\sin(\theta/2)$, where θ is the scattering angle. In this case, from the general expression for the phonon mean free path (see, e.g., [9]), one can get

$$l_k^{-1} = \frac{VNk}{(2\pi\hbar v_s)^2}\int_0^{2\pi} \mathrm{d}\phi' \int_{-\infty}^{\infty} \mathrm{d}k_z' \,\overline{|\langle \boldsymbol{k}|U(r)|\boldsymbol{k}'\rangle|^2}(1-\cos\theta), \tag{4}$$

where N is the number of identical defects (WDDs or WDLs), $v_s = \omega/k$ is the sound velocity. The bar in equation (4) denotes the averaging over α in equations (2) and (3). Assuming that a phonon is incident along the k_x-axis ($\boldsymbol{k} = k\boldsymbol{e}_x$), and using the cylindrical coordinates in the momentum space $(k_\perp, \phi', k_z)$, one can express θ in terms of ϕ' as $1 - \cos\theta = 1 - \sqrt{1-(k_z'/k)^2}\cos\phi'$.

Combining equations (2) and (3) (after averaging over α) with equation (4), we find the mean free paths for WDDs and WDLs:

$$l_{WDD}^{-1} = \frac{4n_d B}{k^2}\int_0^1 \mathrm{d}z\,\frac{\sin^2(zkd)}{z^2}\int_0^{2\pi}\frac{\mathrm{d}\phi'}{1-\sqrt{1-z^2}} \times \left(1 - J_0\left(2Lk\sqrt{2 - z^2 - 2\sqrt{1-z^2}\cos\phi'}\right)\right), \tag{5}$$

$$l_{WDL}^{-1} = n_d R^4 k^2 B\pi^2 \int_0^1 \mathrm{d}z \int_0^{2\pi}\mathrm{d}\phi'\,\frac{1-\sqrt{1-z^2}\cos\phi' - z^2/2}{1-\sqrt{1-z^2}\cos\phi'} \times J_2^2\left(Rk\sqrt{2-z^2-2\sqrt{1-z^2}\cos\phi'}\right), \tag{6}$$

where $z = k_z'/k$, $B = (\nu\gamma)^2(1-2\sigma)^2/(1-\sigma)^2$, $n_d = N/V$ is the total density of defects in a sample. Figures 1 and 2 illustrate the dependences of l_k calculated numerically from equations (5) and (6) for WDDs and WDLs, respectively. One can clearly see the existence of three distinct regimes of scattering in the case of WDDs, and two regimes for circular WDLs over a wide range of frequencies.

To calculate κ with l_k from equations (5) and (6) we use the well-known kinetic formula

$$\kappa = \frac{k_B^4 T^3}{2\pi^2\hbar^3 v_s^2}\int_0^{\theta/T}\frac{x^4 \mathrm{e}^x}{(\mathrm{e}^x - 1)^2} l(x)\,\mathrm{d}x, \tag{7}$$

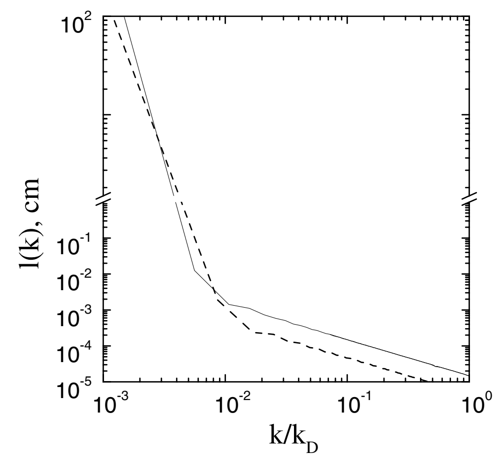

Figure 2. The phonon mean free path l_{WDL} due to scattering on static strain fields of circular WDLs as a function of reduced wavevector k/k_D for the following parameters: $R = L = 2 \times 10^{-6}$ cm, $\nu = 0.1$, $v_s = 4 \times 10^5$ cm s^{-1}. The dashed curve represents the mean free path for uniaxial disclination dipoles.

where $x = \hbar k v_s / k_B T$, $\Theta = \hbar \omega_{max}/k_B$, and the specific heat capacity is chosen in the standard Debye form. We have restricted ourselves to considering thermal phonons with $T \ll \Theta$, where defects are of most importance [14].

3. Results and discussion

In our previous paper [10], where equation (5) was analysed in the limit $d \to \infty$, we showed that a change in behaviour of l_{WDD} occurs when $\lambda \sim 2L$. It was found that for long wavelengths, $l_{WDD} \sim k^{-1}$, while for $\lambda < L$, $l_k \to$ constant. For finite WDDs, there is an additional linear parameter, which is a dipole length $2d$. The analysis of equation (5) shows that the second crossover at low temperatures occurs due to appearance of two regimes of scattering: $kd \gtrsim 1$ and $kd \lesssim 1$. Thus, for finite WDDs we can distinguish the following regimes of scattering:

(i) the high-frequency limit $kd \gtrsim 1$ and $kL \gtrsim 1$ which leads to $l_k \to$ constant;
(ii) $kd \gtrsim 1$ but $kL \lesssim 1$, producing $l_k \sim k^{-1}$; and finally
(iii) for both $kd \lesssim 1$ and $kL \lesssim 1$, we have $l_k \sim k^{-2}$ at low frequencies.

In the special case of $d = L$, only two regimes (with $l_k \sim k^{-2}$ and $l_k \to$ constant) are realized.

In contrast to the case for WDDs, for WDLs we have only a linear parameter R, and, as the result, two regimes of scattering: $kR \gtrsim 1$ and $kR \lesssim 1$. In the long-wavelength limit $kR \gtrsim 1$, the mean free path l_{WDL} increases even more sharply than l_k for the uniaxial dipole ($l_k \sim k^{-5}$) and for a point impurity ($l_k \sim k^{-4}$) (see figure 2). From equation (6) in the limit $k \to 0$, we obtain $l_k \sim k^{-6}$. Thus, a circular WDL is a more self-screened system compared to disclination dipoles (especially to the case considered here of biaxial WDDs whose large strain fields behave like $1/r$). In the opposite limit of short waves ($kR \gtrsim 1$), the phonon scattering due to WDLs behaves like that for edge dislocations where $l_k \sim k^{-1}$. According to equation (7), the above-mentioned behaviour of l_k for finite WDDs results in an extra low-temperature regime with $\kappa \sim T$ ($T < 1$ K; see figure 3), in addition to $\kappa \sim T^2$ and $\kappa \sim T^3$ regimes.

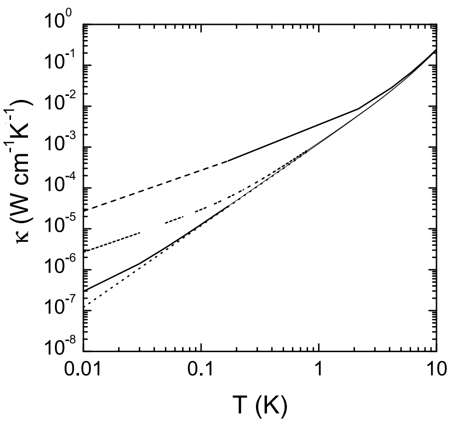

Figure 3. Thermal conductivity versus temperature calculated according to (7) with l_{WDD} from (5) for $d = \infty$ (dotted curve), $d = 10^{-4}$ cm (solid curve), $d = 10^{-5}$ cm (long-dashed curve), $d = 10^{-6}$ cm (dashed curve). The parameter set is the same as in figure 1; $\Theta = 350$ K.

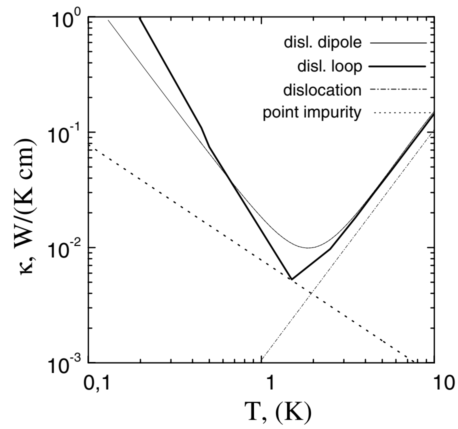

Figure 4. Thermal conductivity versus temperature calculated according to (7) with l_{WDL} from (6). The parameter set is the same as in figure 2; $\Theta = 350$ K. The curves calculated for a dislocation, uniaxial disclination dipole, and point impurity are depicted for comparison.

The dislocation-like behaviour ($\kappa \sim T^2$) takes place for circular WDLs as well as for biaxial WDDs, and infinite uniaxial dipoles above some T^* which is the point of the minimum in $\kappa(T)$ (see figure 4). This behaviour can be explained by an increase in the number of short-wave phonons involved in the local heat transfer from one phonon to another. This process proceeds more rapidly than the phonon scattering by the static strain fields of circular WDLs (or both kinds of WDD), which exhibits a dislocation nature. When $T < T^*$, κ increases drastically (as $\kappa \sim T^{-3}$) with T decreasing ($\kappa \sim T^{-2}$ in the case of uniaxial WDDs). This rise of κ corresponds to the increase in the mean free path ($l_k \sim k^{-6}$ when $k \to 0$) which is the result of the strong localized strain fields near the core of circular WDLs or uniaxial WDDs. Near T^*, phonons with wavelength comparable to the characteristic size of the defect ($kR \sim 1$) are predominantly excited, leading to the strong scattering at the boundary of the defect.

To summarize, in contrast to [8, 10], where infinite biaxial WDDs have been considered, this paper describes a study of the finite biaxial WDD-induced as well as circular WDL-induced phonon scattering within the deformation potential approach. The results obtained have a clear physical meaning. Indeed, both defects have physical linear parameters ($2L$ and d for WDDs, and R for WDLs) which govern the character of the phonon scattering. A strong phonon scattering due to the strain fields of these defects appears when $\lambda \sim 2L$, d, and R. The observed behaviour of the thermal conductivity κ is unique and can serve as indirect evidence of the existence of circular WDLs and WDDs in semiconducting materials. Note that for real materials containing these defects, the situation can be somewhat different due to the existence of other sources of scattering (e.g. boundary scattering, phonon–phonon Umklapp processes). Calculations of $\kappa(T)$ accounting for other sources of scattering will be performed in the near future.

Acknowledgments

This work was supported by the Russian Foundation for Basic Research under Grant No 02-02-16860, and the Heisenberg–Landau programme.

References

[1] Labush R and Schröter W 1980 *Dislocations in Solids* ed F R N Nabarro (Amsterdam: North-Holland) ch 20
[2] Gantmakher V F and Levinson Y B 1987 *Carrier Scattering in Metals and Semiconductors* (Amsterdam: North-Holland)
[3] Muellner P and Pirouz P 1997 *Mater. Sci. Eng.* A **233** 139
[4] Sadoc J F 1982 *Phil. Mag.* B **45** 467
[5] Osipov V A and Krasavin S E 1995 *J. Phys.: Condens. Matter* **7** L95
[6] Krasavin S E and Osipov V A 1997 *Phys. Lett.* A **236** 245
[7] Romanov A E and Vladimirov V I 1983 *Phys. Status Solidi* **78** 11
[8] Krasavin S E and Osipov V A 2001 *J. Phys.: Condens. Matter* **13** 1023
[9] Ziman J M 1960 *Electrons and Phonons: the Theory of Transport Phenomena in Solids* (Oxford: Clarendon)
[10] Osipov V A and Krasavin S E 1998 *J. Phys.: Condens. Matter* **10** L639
[11] Cohn J L, Nolas G S, Fessatidas V, Metcalf T H and Slack G A 1999 *Phys. Rev. Lett.* **82** 779
[12] de Wit R 1973 *J. Res. NBS* A **77** 607
[13] Kuo H H and Mura T 1972 *J. Appl. Phys.* **43** 1454
[14] Carruthers P 1961 *Rev. Mod. Phys.* **33** 92